

# Analysis of New Anisotropic Conductive Film (ACF)

Chao-Ming Lin, Win-Jin Chang, and Te-Hua Fang

**Abstract**—This paper designs a new multilayered particle anisotropic conductive film (ACF) compound. Using the particle-reinforced composite model and probability theory, the novel ACF compound is compared with three traditional ACFs having the same particle volume fraction. The particle-reinforced model applies the concept of bonded and debonded structures in the interfaces between the adhesive resin and the particles. The elastic modulus of the particle-reinforced ACF is a function of the particle volume fraction and the bonded condition. In the failure model, probability theory is used to calculate the probability of opening and bridging. The volume fraction of the conductive particles plays an important role in determining the optimal ACF design. The current results indicate that the flip chip packaging performed using the novel multilayered particle ACF compound (particles distributed in the top/bottom surface layers) exhibits superior particle-reinforcement properties and a lower failure probability than traditional ACFs. The improved understanding of reinforcement mechanisms and failure probability developed by this study facilitates the enhanced design of novel ACF compounds.

**Index Terms**—Anisotropic conductive film (ACF), bridging, flip chip packaging, opening, particle-reinforced composite, probability.

## I. INTRODUCTION

**F**LIP CHIP packaging using anisotropic conductive film (ACF) has evolved into a key technology for the fine-pitch interconnections required in compact electronic products. The ACF compound consists of adhesive resins and conductive metallic or metal-coated polymer particles. ACF has been widely used over the past decade in packaging technologies for flat panel displays (FPDs), such as liquid crystal displays (LCDs), and for attaching bare chips to both flexible and rigid substrates. ACF provides unidirectional conductivity in the vertical, i.e.,  $z$ -axis, direction. This directional conductivity is achieved by applying a relatively low volume fraction loading to the conductive particles. Fig. 1 presents a schematic illustration of a typical cross section of an ACF assembly. The low volume fraction loading, which is insufficient to cause interparticle contact, prevents conductivity in the pitch direction (bridging) [1], [2]. Recently, the use of LCDs has become widespread in various display applications, including

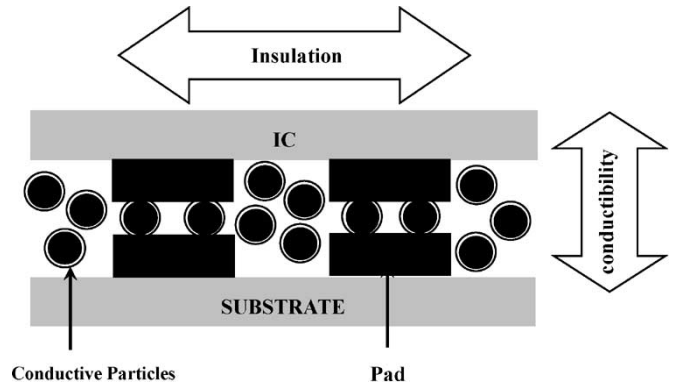


Fig. 1. Schematic illustration of ACF flip chip joint showing insulation and conductivity properties.

notebooks, monitors, TVs, 3C products, etc. The ACFs used in interconnection technologies play an important role in the packaging of LCD modules. The packaging technology should provide a high resolution, be lightweight and thin, and enable a reduced consumption. In a typical ACF joint, the volume fraction of the filler conductive particles is generally specified between 5% and 10% to prevent direct metallic content between the pads and to suppress bridging. ACF packaging technology is highly suitable for small pitch assemblies such as those found in flip chip technology. Generally, ACF joint technology provides a number of advantages, including: 1) fine pitch capability; 2) low-temperature processing capability (resulting in reduced thermal stress during processing); 3) low-cost flexible processing; 4) avoidance of lead or other toxic metals; and 5) compatibility with a wide range of surfaces [3]. The disadvantages in ACF processing include the following: 1) it has a short life for use after preheating; 2) it is easily broken, because the film is both hard and thin; and 3) it is expensive.

Intensive research and development work has been carried out in the field of flip chip and chip-on-glass (COG) technology using ACF as an alternative to traditional soldering methods [4], [5].

This paper investigates the volume fraction effect of the conductive particles on the particle-reinforcement properties and failure tendencies of a novel multilayered particle ACF. The novel ACF (referred to henceforth as ACF-New) is compared with three traditional ACFs (referred to hereafter as ACF-I, ACF-II, and ACF-III, respectively). A basic assumption is made that the novel ACF and the traditional ACFs have the same average particle volume fraction. The four ACFs considered in the study are presented in Fig. 2. Meanwhile, Fig. 3 provides an illustration of the desired conductive adhesive packaging in an ACF assembly, and indicates the normal, bridging and opening cases.

Manuscript received May 17, 2005; revised June 15, 2005. This work was supported by the National Science Council R.O.C. under Grants NSC 92-2212-E-274-004 and NSC 93-2212-E-274-007.

C.-M. Lin is with the Department of Mechanical Engineering, WuFeng Institute of Technology, Chia-Yi 621, Taiwan, R.O.C. (e-mail: cmlin@mail.wfc.edu.tw).

W.-J. Chang is with the Department of Mechanical Engineering, Kun-Shan University, Tainan 710, Taiwan, R.O.C.

T.-H. Fang is with the Institute of Mechanical and Electromechanical Engineering, National Formosa University, Yunlin 632, Taiwan, R.O.C.

Digital Object Identifier 10.1109/TDMR.2005.860557

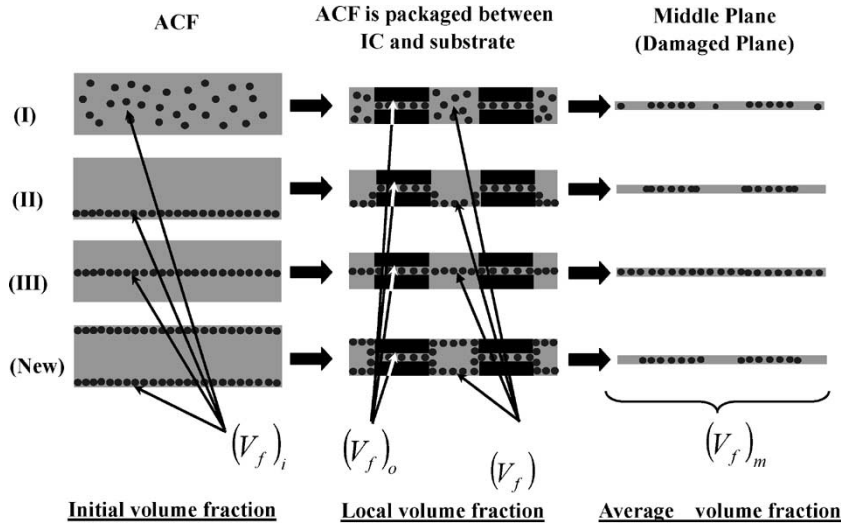


Fig. 2. Schematic illustration of traditional ACFs (I, II, and III) and novel multilayered particle ACF.

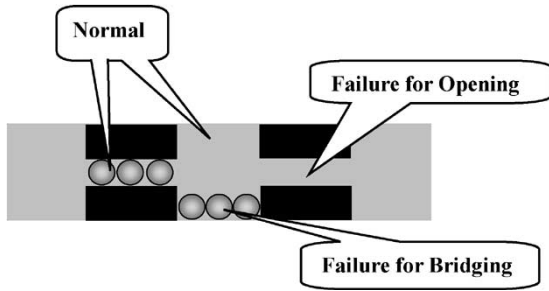


Fig. 3. Normal, bridging, and opening conditions in ACF assembly.

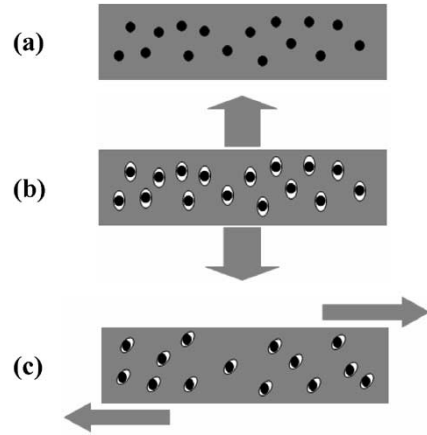


Fig. 4. Schematic illustration of microdamage in particulate composite subjected to: (a) uniaxial tension or shear (bonded); (b) uniaxial tension (debonded); and (c) shear (debonded).

II. PARTICLE-REINFORCEMENT EFFECT IN ACF ASSEMBLY FOR BONDED AND DEBONDED STRUCTURES

Depending on the relative stiffnesses and strengths of the two constituent materials and the interface strength, damage and cracks may occur at the interface between the particles and the cured matrix. In the present study, debonding of the particle/matrix interface is the leading cause of damage in the ACF assembly. The particles are assumed to be spherical in shape. Fig. 4 shows the bonded and debonded situations that arise during tension and shear loading.

In general, only a single layer of conductive particles exists between the two adherents in anisotropy configurations. These conductive particles establish a mechanical contact between the pads, while the polymer binder supplies the tension or shear loading.

The modulus of the composite, matrix, and reinforced particles is governed by the rule of the mixtures. The general formulation for the elastic modulus of the composite is expressed by

$$E_c = V_f E_p + (1 - V_f) E_m \tag{1}$$

where  $E_c$  is the elastic modulus of the composite,  $E_p$  is the elastic modulus of the conductive particles,  $E_m$  is the elastic

modulus of the adhesive resin, and  $V_f$  is the volume fraction of the conductive particles in the adhesive resin.

If the particles are considered to be debonded, (1) can be rewritten as

$$E_c = V_f(1 - \phi) E_p + (1 - V_f) E_m \tag{2}$$

where  $\phi$  is the fraction of the particles that are debonded.

In a specified volume fraction, the particle-reinforcement effect is dominated by the debonded fraction  $\phi$ . The microstructure of the particle/matrix interface must be measured experimentally. The elastic modulus of reinforced composites can be evaluated by tension testing. If  $E_c$  is equal to  $E_m$ , the debonded fraction  $\phi$  can be formulated as  $1 - (E_m/E_p)$ . It is important that the strength of the particle/matrix interface be precisely controlled in order to reduce the debonded fraction, thereby improving the strength of the particle-reinforced ACF and enhancing the quality of the integrated circuit (IC)/substrate structure.

### III. INVESTIGATING OPENING AND BRIDGING USING PROBABILITY THEORY

#### A. Opening Circuit Analysis Using Poisson Distribution

In ACF assemblies, the absence of particles on a pad will result in an open circuit. Therefore, when investigating these assemblies, it is important to have some understanding of the number of particles located on each pad. If it is assumed that the average number of particles on the pads is much smaller than the general crowding number (many particles on a pad), the Poisson distribution can be used to estimate the probability of  $n$  particles existing on a pad [6], i.e.,

$$P(n) = \frac{\mu_1^n e^{-\mu_1}}{n!} \quad (3)$$

$$V_f = \frac{\text{particles volume}}{\text{gap volume}} = \frac{\mu_1 \cdot \frac{4}{3}\pi r^3}{2rl^2} \quad (4a)$$

$$\mu_1 = \frac{3l^2 V_f}{2\pi r^2} \quad (4b)$$

where  $P(n)$  is the probability of there being  $n$  particles located on the pad;  $\mu_1$  is the average number of particles on the pads in the current direction;  $V_f$  is the volume fraction of particles in the resin;  $l$  is the length of the square pad; and  $r$  is the particle radius.

The probability of an open circuit occurring between the pads in the current direction can be expressed as

$$P_{\text{opening}}(0) = e^{-\mu_1} = e^{-\frac{3l^2 V_f}{2\pi r^2}}. \quad (5)$$

#### B. Bridging Circuit Analysis Using Box Model

The probability of a short circuit occurring between the pads in the pitch direction [6] can be expressed as

$$P_{\text{bridging}} = 1 - \left(1 - \mu_2 \frac{d}{2r}\right)^{\frac{hl}{4r^2}} \quad (6)$$

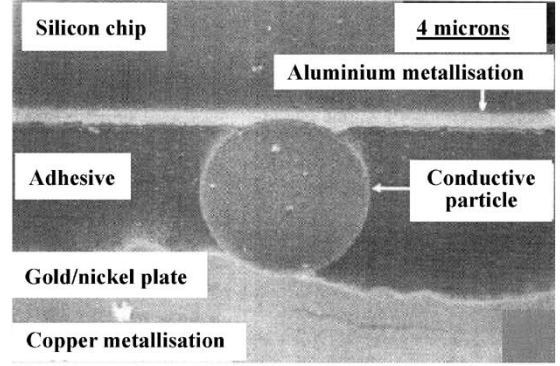
where  $\mu_2$  is the average number of boxes (including particles) between the pads in the pitch direction,  $d$  is the distance between the pads,  $h$  is the pad height,  $l$  is the square pad width, and  $r$  is the radius of the conductive particles.

The volume fraction of the particles between the pads in the pitch direction can be derived from

$$V_f = \frac{k \left(\frac{4\pi r^3}{3}\right)}{N(2r)^3} = \frac{k\pi}{6N} \quad (7)$$

$$\mu_2 = \frac{k}{N} = \frac{6V_f}{\pi} \quad (8)$$

where  $N$  is the number of cubic boxes in the region between the pads,  $k$  is the number of cubic boxes containing particles in the region between the pads,  $(\frac{4\pi r^3}{3})$  is the volume of each particle, and  $(2r)^3$  is the volume of each cubic box. The conductive particle is assumed to be a spherical particle in



Source:

[http://www.ewh.ieee.org/mm/cpmt/adhesives/lectnote/ECA\\_course\\_intro\\_1.pdf](http://www.ewh.ieee.org/mm/cpmt/adhesives/lectnote/ECA_course_intro_1.pdf), Page.7

Fig. 5. Spherical conductive particle between the IC/substrate.

the calculation. Fig. 5 shows a spherical conductive particle between the IC/substrate in an actual cross section.

Mannan *et al.* [6] established a box model to estimate the probability of bridging between the pads. To calculate this bridging probability, the proposed box model considered only the shortest distance between the pads in the pitch direction. The probability of a short circuit between the pads in the pitch direction [6] is given by

$$P_{\text{bridging}} = 1 - \left(1 - \left(\frac{6V_f}{\pi}\right)^{\frac{d}{2r}}\right)^{\frac{hl}{4r^2}} \quad (9)$$

where  $V_f$  is the volume fraction of the conductive particles,  $d$  is the distance between the pads,  $h$  is the pad height,  $l$  is the square pad width, and  $r$  is the radius of the conductive particles.

#### C. Failure Analysis

Failure probability can be defined in terms of the probability of either shorting or bridging. Hence, the failure probability can be expressed as

$$P_{\text{opening}\cup\text{bridging}} = P_{\text{opening}} + P_{\text{bridging}} - P_{\text{opening}\cap\text{bridging}} \quad (10)$$

where  $P_{\text{opening}\cup\text{bridging}}$  is the probability of opening or bridging and  $P_{\text{opening}\cap\text{bridging}}$  is the probability of opening and bridging.

If opening and bridging are independent events, the overall failure probability  $P_{\text{opening}\cup\text{bridging}}$  can be expressed as

$$P_{\text{opening}\cup\text{bridging}} = P_{\text{opening}} \cdot P_{\text{bridging}} \quad (11)$$

Substituting (11) into (10), and defining the failure probability in the IC/substrate assembly as  $P_{\text{opening}\cup\text{bridging}}$ , the failure probability can be formulated as

$$\begin{aligned} P_{\text{failure}} &= P_{\text{opening}\cup\text{bridging}} \\ &= P_{\text{opening}} + P_{\text{bridging}} - P_{\text{opening}} \cdot P_{\text{bridging}}. \end{aligned} \quad (12)$$

TABLE I  
INITIAL VOLUME FRACTION (IN THE PARTICLES LAYER), AVERAGE VOLUME FRACTION (IN THE MIDDLE PLANE), LOCAL VOLUME FRACTION ON THE PADS (FOR OPENING), AND LOCAL VOLUME FRACTION BETWEEN THE PADS (FOR BRIDGING) FOR FOUR ACFs

Type \ Property	$(V_f)_i$	$(V_f)_m$	$(V_f)_o$	$(V_f)_b$
ACF-I	$f$	$f$	$f$	$f$
ACF-II	$\frac{t}{2r}f$	$\frac{l^2}{(l+d)^2+4hl} \cdot \frac{t}{2r}f$	$\frac{(l+d)^2}{(l+d)^2+4hl} \cdot \frac{t}{2r}f$	$\frac{(l+d)^2}{(l+d)^2+4hl} \cdot \frac{t}{2r}f$
ACF-III	$\frac{t}{2r}f$	$\frac{t}{2r}f$	$\frac{t}{2r}f$	$\frac{t}{2r}f$
ACF-New	$\frac{t}{4r}f$	$\frac{l^2}{(l+d)^2+4hl} \cdot \frac{t}{2r}f$	$\frac{(l+d)^2}{(l+d)^2+4hl} \cdot \frac{t}{2r}f$	$\frac{(l+d)^2}{(l+d)^2+4hl} \cdot \frac{t}{4r}f$

Initial thickness:  $t$ ; Particle radius:  $r$ ; Total volume fraction:  $f$ ; Pad height:  $h$ ; Pad length:  $l$ ;  
Pitch:  $d+l$ ; Final thickness:  $2(h+r)$   
 $(V_f)_i$ : Initial volume fraction  
 $(V_f)_m$ : Average volume fraction in the middle plane  
 $(V_f)_o$ : Local volume fraction on the pads for estimating the opening effect  
 $(V_f)_b$ : Local volume fraction between the pads for estimating the bridging effect

Substituting (5) and (9) into (12) yields

$$P_{\text{failure}} = e^{-\frac{3l^2V_f}{2\pi r^2}} + \left\{ 1 - \left[ 1 - \left( \frac{6V_f}{\pi} \right)^{\frac{d}{2r}} \right]^{\frac{hl}{4r^2}} \right\} - e^{-\frac{3l^2V_f}{2\pi r^2}} \cdot \left\{ 1 - \left[ 1 - \left( \frac{6V_f}{\pi} \right)^{\frac{d}{2r}} \right]^{\frac{hl}{4r^2}} \right\}. \quad (13)$$

The minimum failure probability is then found by differentiating (13) with respect to the volume fraction, i.e.,

$$\frac{d(P_{\text{failure}}(V_f))}{dV_f} = 0. \quad (14)$$

Equation (14) can be solved using numerical methods. The solution  $V_f$  gives the optimal value of the volume fraction, i.e., the value that results in the lowest probability of failure.

#### D. Computing the Volume Fraction After Packaging

An important assumption made in this study is that the surface layer of the ACF after touching the IC/substrate is uniformly distributed over the entire surface (spread uniformly over the pads surfaces, the IC and the substrate).

**Average Volume Fraction for Middle Plane (Damaged Plane):** To analyze the shear and tensile failure, the damaged plane is assumed in the middle plane. Hence, the volume fractions of the middle plane for four ACFs must be estimated by the average volume. The volume of particles in the middle plane is divided by the middle layer volume. Fig. 2 shows the matrix with particles in the middle plane layer for four ACFs. The average volume fractions are shown in the Table I. The

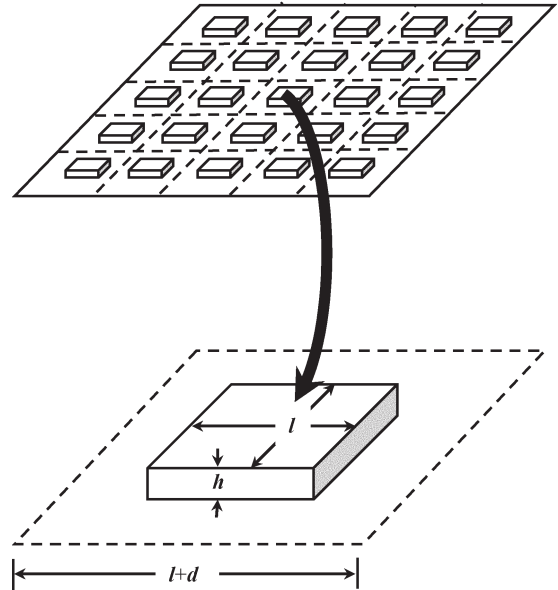


Fig. 6. Unit structure is outlined from the pad array substrate.

results show that ACF-II and ACF-New have the same average volume fraction  $(l^2/((l+d)^2+4hl)) \cdot (tf/2r)$  (which is equal to  $((l+d)^2/((l+d)^2+4hl)) \cdot (tf/2r) \cdot (l^2/(l+d)^2)$ ), where  $t$  is the initial thickness of the ACF and  $f$  is the total volume fraction.

**Local Volume Fraction for Opening and Bridging Analysis:** In Fig. 6, the unit structure is plotted in the lower figure and the total surface area is equal to  $(l+d)^2+4hl$ . The original ACF area  $(l+d)^2$  will be expanded into the total surface area of the unit structure  $(l+d)^2+4hl$ , and the volume fraction is changed from  $(tf/2r)$  to  $((l+d)^2/((l+d)^2+4hl)) \cdot (tf/2r)$ . In the ACF-New case, the initial volume fraction is equal to

TABLE II  
LOCAL VOLUME FRACTION (FOR OPENING AND BRIDGING), OPENING PROBABILITY, BRIDGING PROBABILITY,  
AND FAILURE PROBABILITY FOR FOUR REPRESENTATIVE ACF CASES

Type \ Property	$(V_f)_o$	$(V_f)_b$	$P_{opening}$	$P_{bridging}$	$P_{failure}$
ACF-I	0.005	0.005	0.384839	0	0.384839
ACF-II	0.333	0.333	2.43E-28	0.103133	0.103133
ACF-III	0.5	0.5	3.37E-42	0.999953	0.999953
ACF-New	0.333	0.1665	2.43E-28	0.000106	0.000106

$t=1000, l=100, d=100, h=50, r=5$  (unit: micron) Initial volume fraction=0.005

$(tf/4r)$  and the local volume fraction is equal to  $((l+d)^2 / ((l+d)^2 + 4hl)) \cdot (tf/4r)$ . Because the particles in the ACF-New case are divided into upper/lower layers, the opening volume fraction between the gap is still kept in  $((l+d)^2 / ((l+d)^2 + 4hl)) \cdot (tf/2r)$  and the bridging volume is reduced as  $((l+d)^2 / ((l+d)^2 + 4hl)) \cdot (tf/4r)$ . The estimation of the volume fractions for four ACF are listed in the Table I. Table I shows the average volume fraction of the particles in the middle plane, while Table II shows the local volume fraction of the particles in the particle layer.

#### IV. RESULTS AND DISCUSSIONS

In this study, the distance between the IC/substrate pads is a monolayer of spherical particles. In the close-packed case, these particles are in the form of a hexagonal array. The close-packed unit cell for such layers comprises a central particle and six  $120^\circ$  segments of other particles. Such a rect-six-polygonal unit cell contains three spherical particles, and the volume ratio of the three particles/unit cell is 0.6. Hence, the maximum volume fraction in the close-packed case is equal to 0.6. Consequently, the case where  $V_f > 0.6$  cannot exist in the analysis that follows [7].

##### A. Particle-Reinforcement Effect

In the present study, there are basically two failure modes capable of destroying the ACF assembly, namely tension and shear. Generally, tension is caused by increasing the separation between the IC and the substrate, while shear failure arises as a result of bending. The effective volume fractions in the middle plane for all four ACF cases considered in the current investigation are listed in Table I. It is assumed that the particle layers are uniformly distributed across the contact areas. Hence, the local volume fraction will be smaller than the initial volume fraction. In the present analysis, the average volume fraction is defined as the effective volume fraction in the middle plane. In this study, the effective volume fraction is increased in order to reinforce the ACF assembly and form a perfect bonding between the particles/matrix. An imperfect bonding will result in a loss of strength. The effects of increasing the volume fraction on the elastic modulus in the bonded and debonded cases are presented in Fig. 7. Some cases between perfect and imperfect bonding can be indexed by the debonded fraction  $\phi$ . Different debonded fractions cause the particle-reinforcement

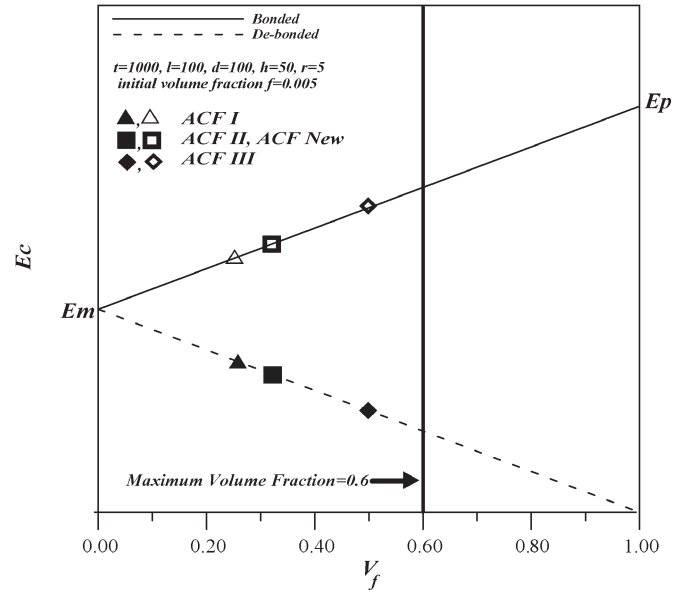


Fig. 7. Elastic modulus for different volume fractions in bonded and debonded conditions.

properties to vary between 0 and  $E_p$ . In other words, the debonded fraction  $\phi$  is equal to  $1 - (E_m/E_p)$  and  $E_c$  is equal to  $E_m$ . The variation of the elastic modulus with the volume fraction for different debonded fractions is presented in Fig. 8. The strengths of the matrix and particles can be chosen in adaptive proportions in order to enhance the strength of the ACF assembly composite. Fig. 9 plots the variation of  $E_c/E_p$  with  $E_m/E_p$  for different debonded fractions.

##### B. Failure Analysis

The probability theory used in the current failure analysis provides an accurate estimation of the optimal local particle content required to prevent opening and bridging failures. In comparing the performance of the four ACFs, it is assumed that the average volume fraction is the same in each case. In ACF-I, the volume fraction in the initial and packaged condition is given by  $f$  in both cases. In ACF-II, the particles are concentrated in the lower layer, and the local volume fraction is  $(tf/2r)$ . Meanwhile, in ACF-III, the particles are concentrated in the middle plane, and the local volume fraction is again given by  $(tf/2r)$ . Finally, in ACF-New, the particles are

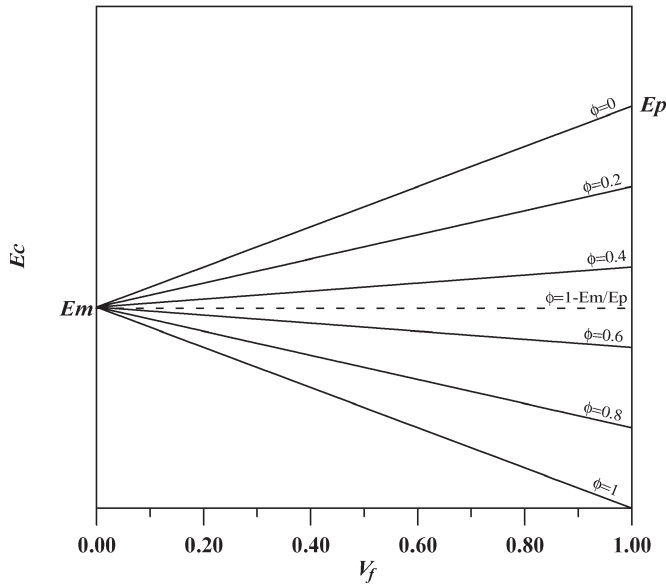


Fig. 8. Variation of elastic modulus with volume fraction for different debonded fractions.

separated into upper/lower layers and the local volume fraction is  $(tf/4r)$ . Hence, the volume fraction following packaging can be calculated in terms of the geometric parameters  $l, d, h, t,$  and  $r$ . The corresponding formulations are listed in Table I. Taking a real case of  $t = 1000, l = 100, d = 100, h = 50, r = 5 \mu\text{m}$ , and a total volume fraction of 0.005, Table II presents local volume fraction (for opening and bridging), opening probability, bridging probability, and failure probability for four representative ACF cases. The results indicate that the packaged volume fraction of ACF-I ( $V_f = 0.005$ ) is the smallest of the four cases. In ACF-New, the local volume fractions are found to be 0.333 on the pads and 0.1665 between the pads. Furthermore, the results show that the opening probability of ACF-New ( $2.43\text{E-}28$ ) is lower than ACF-I and ACF-III, while the bridging probability is equal to  $1.06\text{E-}04$ . Although the bridging probability of ACF-New is greater than that of ACF-I, the overall failure probability of ACF-New is the smallest of the four ACFs. Hence, the novel multilayered particle ACF is shown to be an excellent anisotropic conductive film. Generally speaking, the opening effect is a function of the particle number and volume fraction with the exponential decay, and the opening probability is small and strongly related to the particle number.

C. Advantages of Novel ACF

The advantages of the novel multilayered particle ACF can be summarized as follows:

- 1) The developed ACF is more convenient to manufacture than traditional ACFs. The conductive particles can be spread randomly on the pads, the IC, and the substrate.
- 2) In the ACF structure, the strength in the middle damaged plane is elevated by the particle-reinforcement effect.
- 3) Regarding the opening effect, the probability of an opening circuit can be effectively reduced by specifying a high-density conductive particle layer.

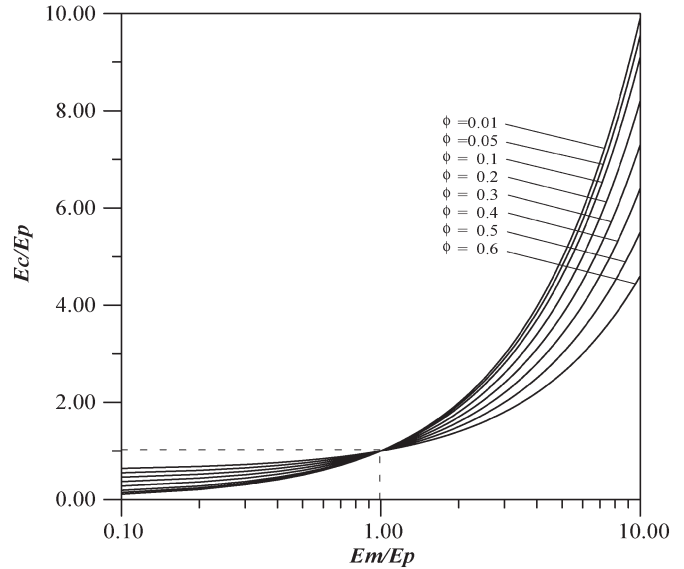


Fig. 9. Variation of elastic modulus (particles, matrix, and composite) for different debonded fractions.

- 4) Considering the bridging effect, the particle layer is divided into upper/lower layers with the result that the volume fraction is reduced. Hence, the probability of bridging (shorting) between the particles is reduced.
- 5) Regarding the heat transfer, the upper/lower surfaces include embedded particles and form a composite layer (particle and matrix). The heat generated in the sealing process is conducted rapidly into/out of the particle-resin layer. Hence, the assembly obtains a uniform temperature distribution, with the result that thermal stress and shrinkage is reduced.

V. CONCLUSION

This paper has investigated the particle-reinforcement strength and failure probability of a novel multilayered ACF for flip chip packaging. The volume fraction of the conductive particles is the key factor controlling the basic properties of the ACF composite, including its elastic modulus and the failure probability. In a perfect bonding, a high volume fraction of particles in the ACF assembly increases the strength of the composite material and reduces the opening probability, but increases the bridging probability. However, the novel ACF designed in this study achieves a high volume fraction of particles in the local region. This enhances the strength of the ACF assembly, while simultaneously reducing the overall failure probability.

REFERENCES

- [1] R. R. Tummala and E. J. Rymaszewski, *Microelectronics Packaging Handbook*. New York: Van Nostrand Reinhold, 1989, pp. 366–391.
- [2] J. Lau, *Low Cost Flip Chip Technologies*. New York: McGraw-Hill, 1996, pp. 1–17.
- [3] J. Liu, *Conductive Adhesives for Electronics Packaging*. London, U.K.: Electrochemical Publications Ltd., Jun. 1999.
- [4] H. Date *et al.*, “Anisotropic conductive adhesive for fine pitch interconnections,” in *Proc. Int. Symp. Microelectronics*, Boston, MA, 1994, pp. 570–575.

- [5] A. Torri, M. Takizawa, and K. Sasahara, "Development of flip chip bonding technology using anisotropic conductive film," in *Proc. 9th Int. Microelectronics Conf.*, St. Petersburg, Russia, 1996, pp. 324–327.
- [6] S. H. Mannan, D. J. Williams, D. C. Whalley, and A. O. Ogunjimi, "Models to determine guidelines for the anisotropic conducting adhesives joining process," in *Conductive Adhesives for Electronics Packaging*, J. Liu, Ed. London, U.K.: Electrochemical Publications Ltd., Jun. 1999, ch. 4.
- [7] D. J. Williams and D. C. Whalley, "The effects of conducting particle distribution on the behaviour of anisotropic conducting adhesives: Non-uniform conductivity and shorting between connections," *J. Electron. Manuf.*, vol. 3, no. 2, pp. 85–94, 1993.



**Chao-Ming Lin** received the M.S. and Ph.D. degrees in mechanical engineering from the National Cheng Kung University, Tainan, Taiwan, in 1993 and 1999, respectively.

He has some publications in the areas of electronic packaging and polymer processing. He is currently with the WuFeng Institute of Technology, Taiwan, as an Associate Professor with research interest in integrated circuit (IC) packaging, injection molding packaging, electrically conductive adhesive/films, polymer packaging composites, etc.



**Win-Jin Chang** received the M.S. and Ph.D. degrees in mechanical engineering from the National Cheng Kung University, Tainan, Taiwan, in 1990 and 1999, respectively.

He is currently a Professor in the Department of Mechanical Engineering at the Kun-Shan University of Technology, Taiwan. His research interests include nanotechnology, heat and mass transfer, and optical engineering.



**Te-Hua Fang** received the M.S. and Ph.D. degrees in mechanical engineering from the National Cheng Kung University, Tainan, Taiwan, R.O.C., in 1995 and 2000, respectively.

He is currently with the National Formosa University, Taipei, Taiwan, as an Associate Professor of the Institute of Mechanical and Electromechanical Engineering and as the Director of the Nanotechnology Laboratory with research interests in nanotechnology, scanning probe microscopy, optoelectronics, and molecular dynamics. He has some publications

in the areas of nanotechnology and semiconductor processing.